Pure Appl. Geophys. 177 (2020), 1781–1800

https://doi.org/10.1007/s00024-019-02336-8

Pure and Applied Geophysics

# Re-evaluation of Seismic Intensities and Relocation of 1969 Saint Vincent Cape Seismic Sequence: A Comparison with the 1755 Lisbon Earthquake

E. Buforn,[1] C. López-Sánchez,[1] L. Lozano,[2] J. M. Martínez-Solares,[2] S. Cesca,[3] C. S. Oliveira,[4] and A. Udías[1]

*Abstract*—Seismic intensity for the February 28, 1969 (Mw = 7.8) earthquake have been re-evaluated using original documents in local archives, such as, contemporary newspapers, council minutes, monographic studies, among other sources for Spain, Portugal and Morocco and answers to macroseismic questionnaires for Morocco. This information is used to plot a new intensity map for the whole region affected by the earthquake: Portugal, Spain and Morocco. The intensity values vary from VIII to IX in the E-W coast of Algarve, southern Portugal, to II–III. Furthermore, we have relocated the hypocentres for main shock and 24 aftershocks using a new 3D crustal velocity model for the Gulf of Cadiz region and a non-linear probabilistic location methodology, most of them previously lacking a depth estimate. The new locations show an E-W distribution of epicenters, with focus located in the uppermost mantle, most of them with depths between 30 and 50 km. No earthquakes have been located at depths shallower than 30 km. A comparison between peak ground accelerations (PGAs) estimated from the observed intensities for the 1969 and the Lisbon 1755 earthquakes, and synthetic PGA values, generated assuming two different scenarios (using the 1969 and 2009 earthquakes) for the 1755 Lisbon event, shows that the observed damage produced by the 1755 earthquake may be better explained assuming a reverse dip-slip mechanism oriented in NE-SW direction, similar to that of the 2009 earthquake, rather than assuming focal mechanism similar to that of the 1969 earthquake.

**Key words:** 1969 earthquake, 1755 Lisbon earthquake, intensity re-evaluation, hypocentral relocation.

## 1. Introduction

The 1969, February 28 $M_w$ = 7.8 earthquake is the largest shock occurred during the instrumental period (1920—present) offshore SW of the Iberian Peninsula, at the plate boundary between Eurasia and Africa and with epicenter close to that assumed for the 1755 Lisbon earthquake. The 1969 event generated a tsunami (about 1 m high), much smaller than that of 1755, reaching SW Iberia (Portugal and Spain) and the Atlantic coast of Morocco. The 1969 earthquake was felt at great part of Iberia and NW Morocco, producing the largest damage along the Atlantic coast of Portugal and Spain. There are several intensity maps for this event, most corresponding only to the intensity values for each country: Portugal, Spain or Morocco. Only a few of them show the seismic intensity for the whole region. In this study, we have carried out a revaluation of the seismic intensities for the 1969 main shock for the whole region, that is Portugal, Spain and Morocco, using original contemporary sources and the EMS-98 scale.

The 1969 earthquake was followed by a seismic sequence lasting several months. However, the epicentral locations of these aftershocks are very poorly, determined due to the low number of seismic stations at the region in that time, all very distant from the epicentral area, the poor azimuthal coverage and the use of 1D structure models for the hypocentral location. Due to these limitations, it was not possible to estimate reliable focal depths for most of these aftershocks. Over the last years, new algorithms using 3D velocity models have been developed for hypocentral determination, which allows improving the location accuracy, especially, with respect the determination of the focal depth. In the second part of

**Electronic supplementary material** The online version of this article (https://doi.org/10.1007/s00024-019-02336-8) contains supplementary material, which is available to authorized users.

[1] Dto de Física de la Tierra y Astrofísica, Universidad Complutense, 28040 Madrid, Spain. E-mail: caroll04@ucm.es

[2] Instituto Geográfico Nacional, Madrid, Spain.

[3] GFZ German Research Centre for Geosciences, 14467 Potsdam, Germany.

[4] Instituto Superior Tecnico/CEris, Universidade de Lisboa, Lisbon, Portugal.

this study, we discuss the relocation of a subset of the largest aftershocks, using a new accurate 3D crustal velocity distribution for the Gulf of Cadiz region (Lozano et al. 2019 under revision) and a non-linear probabilistic location method (NonLinLoc, Lomax et al. 2000). Data used correspond to all the available regional phase data recorded at Spanish, Portuguese and Moroccan stations. We have used the original arrival times, from the Instituto Geográfico Nacional (IGN) Seismic Catalogue, seismic stations bulletins from 1969 to 1970 and included a number of new available phase data information. Following several reliability criteria (a minimum number of stations and of P and S waves arrivals), we have selected 25 earthquakes occurred in the period between February 28 and December 31, 1969. Although the location of these earthquakes is highly influenced by the poor network configuration (all stations are located onshore at epicentral distances larger than 300 km and there is a large azimuthal gap of 240° of stations coverture), the use of a probabilistic approximation and a more realistic 3D crust and upper mantle model provides not only better maximum likelihood hypocentre, but also more accurate focal depths, not available by previous studies.

The 1969 main shock occurred on February 28, at 02 h 40 m 32 s with epicentre located SW of Saint Vincent Cape (35.9850°N, 10.8133°W) and at 20 km depth, (http://www.ign.es/web/ign/portal/sis-catalogo-terremotos). It is located at the plate boundary between Eurasia and Africa, very close to the point where the transition begins from an oceanic and well defined plate boundary to the west to a continental and more diffuse limit to the east (Fig. 1a, b). As a consequence of this transition, the seismicity is more diffuse from 12°W to the east, with several alignment of epicenters (Fig. 1b), corresponding the plate boundary to a wider deformation zone (Buforn et al. 1995). From 12°W to 9°W, we observe several alignments of epicentres that may be correlated with the main geological structures (Martínez-Loriente et al. 2013). A NE-SW distribution of epicentres may be correlated to the Gorringe Bank Fault (GBF), another alignment of epicentres follows a WNW–SES direction and may be associated to the Horsehoe Fault (HF) where the 1969, the 2003 ($M_w$ = 5.3) and the 2007 ($M_w$ = 5.9) earthquakes are located (Fig. 1b). There is a third line of epicentres, along the submarine Saint Vincent Canyon Fault (SVCF) that starts around 36°N, 10°W and runs in a NE-SW direction to the western part of Saint Vincent Cape (SVC) where is located the 2009 earthquake ($M_w$ = 5.5). From 9°W to 7°W the epicentres follow an E-W direction over a wider zone (near 100 km width) following the Guadalquivir Bank (GB), with the seismic activity decreasing as it approach the Spanish coast. In this zone is located the $M_w$ = 6.5, 1964 earthquake (Udías and López Arroyo 1970). A NW-SE minor alignment may be observed from 8°W to 6°W, following the Gulf of Cadiz-Morocco Fault (CGMF) which reaches the interior of Morocco; the largest earthquake located in this zone is the 1960 event ($M_b$ = 6.1). The location of the large 1755 Lisbon earthquake is still a debatable question and several macroseismic epicentres have been proposed based on the distribution of damage, tsunami propagation and other factors (Machado 1966; Moreira 1985; Martínez Solares et al. 1979; Baptista et al. 1998; Zitellini et al. 1999; Vilanova et al. 2003; Martínez Solares and López Arroyo 2004; Grandin et al. 2007; Pro et al. 2013). We use in this study the epicentre proposed by Martínez Solares and López Arroyo (2004), located in proximity to the 2009 event. This epicentre is based on the results obtained from modelling of the tsunami waves generated by the earthquake (Baptista et al. 1998). Further, the intensities distribution for the 2009 earthquake show high values along the south of Portugal (the Algarve N–S coast) and in the Lisbon region, similar to those of the 1755 earthquake (Carranza 2016).

The 1969 shock has been the object of different studies with similar results on focal mechanism: reverse faulting with both nodal planes oriented in approximately E–W direction and horizontal pressure axis oriented in NNW-SSE direction. The focal depth varies from 16 to 33 km (López-Arroyo and Udías 1972; McKenzie 1972; Fukao 1973; Udías et al. 1976; Grimison and Chen 1986, 1988; Buforn et al. 1988; Grandin et al. 2007). The 1964 earthquake, 1969 largest aftershock (1969A in Fig. 1b), 2003 and 2007 events have all similar focal mechanisms. However, the 2009 earthquake, which is located at NE and with similar epicenter of those proposed by

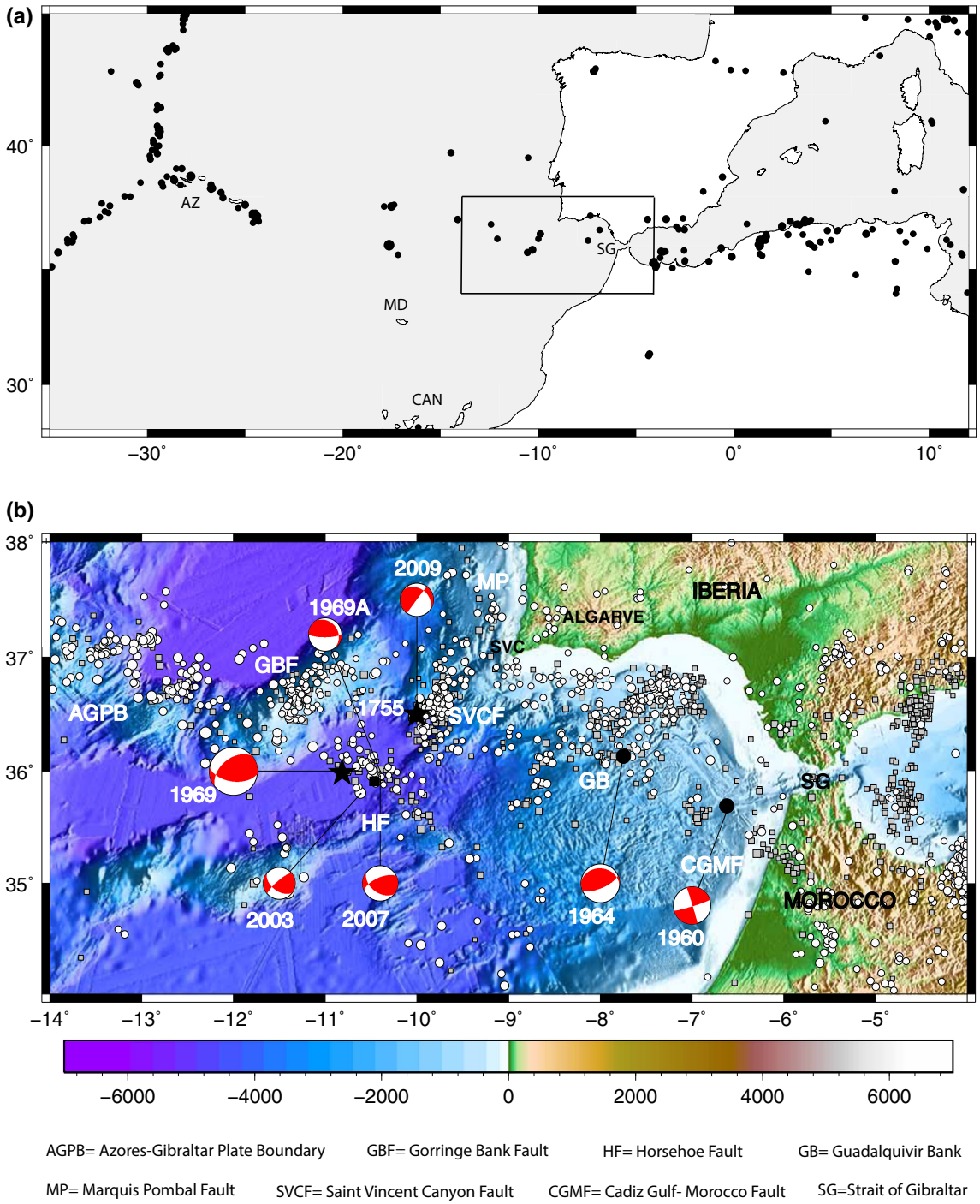


Figure 1

**a** Seismicity along the plate boundary between Eurasia and Africa from the Azores Triple Point to Tunisia for period 1930–2019, M ≥ 5.0. The square corresponds to the region plotted in Fig. 1b. *AZ* Azores, *MD* Madeira, *CAN* Canary Islands, *SG* Strait of Gibraltar. **b** Distribution of epicenters for the period 2000–2019 (M ≥ 3.0) (https://www.ign.es/web/ign/portal/sis-catalogo-terremotos) (white circles h < 40 km, grey squares, h > 40 km) and focal mechanism of largest shocks for this area (Pro et al. 2013). Stars correspond to the 1755 (Martínez Solares and López Arroyo 2004) and 1969 epicenters (https://www.ign.es/web/ign/portal/sis-catalogo-terremotos)

the IGN for the 1755 Lisbon earthquake has a different focal mechanism: dip-slip motion on a vertical plane oriented on NE-SW direction (Stich et al. 2005, 2007; Custodio et al. 2012; Pro et al. 2013). From Fig. 1b we observe a change on focal mechanisms as earthquakes approach the Strait of Gibraltar: for example, the 1960 earthquake shows strike-slip faulting, similar to the recent northern Africa earthquakes: Al-Hoceima 1994 ($M_w = 5.8$), and 2004 ($M_w = 6.2$) and Alboran 2016 ($M_w = 6.4$) (Buforn et al. 2017).

## 2. *Re-evaluation of Intensities for the 1969 Main Shock*

The 1969 shock was felt in great part of the Iberian Peninsula and NW of Morocco, producing damage and losses of human life. There are several intensity maps for this earthquake, but most show the intensities for Portugal, Spain or Morocco separately (Martínez Solares et al. 1979; Moreira 1984; Paula and Oliveira 1996; Cherkaoui 1991; Levret 1991). The intensity map by López-Arroyo and Udías (1972) is the only one covering the whole region. Other maps for the whole region are based on this one (Martínez Solares et al. 1979; Mézcua 1982) or put together joining several maps (Grandin et al. 2007).

For this reason, we have carried out a search of contemporary documents in local and national archives, archives of city halls, churches, etc. in order to find detailed information about the damage produced by this shock. We have used newspapers from Spain (54), Portugal (10), Morocco (3) and France (1), reports from national, regional and local archives for Portugal and Spain and answers to macroseismic questionnaires for Spain (very low number) and Morocco (larger number). In Tables 1, 2 and 3 we have summarized the list of documents used in this paper and assigned a reference to each document. From these documents we have obtained information for more than 640 sites on the three countries including data from as far as Azores, Madeira and Canary Islands. Based on this data we have re-evaluated the seismic intensities at a large number of places using the EMS-98 scale (Table S1). In addition, we have complemented the intensity values with

Table 1

*List of journals used for re-evaluation of intensity for 1969*

| Newspapers Spain | Reference | Newspapers Spain | Reference |
|---|---|---|---|
| ABC (Madrid and Sevilla) | S1 | Ideal | S30 |
| El adelantado de Segovia | S2 | Jaén | S31 |
| El Adelanto | S3 | Lanza | S32 |
| El Alcázar | S4 | Madrid | S33 |
| Área | S5 | Le Monde | S34 |
| Baleares | S6 | Norte de Castilla | S35 |
| Córdoba | S7 | El Noticiero de Cartagena | S36 |
| El correo de Andalucía | S8 | Nueva Rioja | S37 |
| El correo de Zamora | S9 | Odiel | S38 |
| El día | S10 | Proa | S39 |
| Diario de Ávila | S11 | La Provincia | S40 |
| Diario de Burgos | S12 | Pueblo | S41 |
| Diario de Cádiz | S13 | Soria | S42 |
| Diario de Cuenca | S14 | Sur | S43 |
| Diario de Las Palmas | S15 | La tarde | S44 |
| Diario de León | S16 | El telegrama de Melilla | S45 |
| Diario de Navarra | S17 | La Vanguardia | S46 |
| Diario Montañés | S18 | La verdad | S47 |
| Diario Palentino | S19 | La voz de Albacete | S48 |
| Diario popular | S20 | La voz de Almería | S49 |
| Diario regional | S21 | La voz de Asturias | S50 |
| Diario vasco | S22 | La voz de Castilla | S51 |
| Extremadura | S23 | La voz de Galicia | S52 |
| El faro de Ceuta | S24 | La voz del Sur | S53 |
| Faro de Vigo | S25 | Ya | S54 |
| Gaceta del Norte | S26 | | |
| La higuerita | S27 | Macroseismic enqueries | MES |
| Heraldo de Aragón | S28 | | |
| Hoy | S29 | | |
| **Newspapers Portugal** | **Reference** | **Newspapers Morocco** | **Reference** |
| Correio do Sul | P1 | L'opinion | M1 |
| Democracia do sul | P2 | Le petit Marocain | M2 |
| Diario de Lisboa | P3 | La vigie marocaine | M3 |
| Diario do sul | P4 | | |
| Diario Popular | P5 | Macroseismic enqueries | MEM |
| Folha do domingo | P6 | | |
| Jornal do Algarve | P7 | | |
| Noticias d'Evora | P8 | | |
| O Algarve | P9 | | |
| República | P10 | | |
| Povo Algarve | P11 | | |

Table 2

*Local archives used for re-evaluation of intensity for 1969*

| |
|---|
| ADPH: Archivo de la Diputación Provincial de Huelva |
| AMH: Archivo Municipal de Huelva |
| AMIC: Archivo Municipal de Isla Cristina (Huelva) |
| BOOH: Boletín Oficial del Obispado de Huelva |
| BPPH: Biblioteca Pública Provincial de Huelva |
| HBPPC: Hemeroteca de la Biblioteca Pública Provincial de Cádiz |
| HMJF: Hemeroteca Municipal de Jerez de la Frontera (Cádiz) |
| HN: Hemeroteca Nacional |

Table 3

*Local references used for re-evaluation of intensity for 1969*


Alvarez Checa, J., De la Villa Márquez, L. and Mojarro Bayo, A. M. (2002) *Guía de arquitectura de Huelva*. Colegio Oficial de Arquitectos de Huelva, 360 pp

Carrasco Terriza, M. J., Gónzalez, Gómez, J. M., Oliver, A., Pleguezuelo, A., Sánchez Sánchez, J. M. (2006). *Guía artística de Huelva y su provincial*. Fundación José Manuel Lara. Diputación Provincialde Huelva, 632 pp

Díaz Hierro, J. (1975). *Historia de la Merced de Huelva, hoy Catedral de su Diócesis*. Editorial Huelva

Fernández Jurado, J. (1986). *Huelva y su provincia*. Ediciones Tartessos S.L. Volumen I, 325 pp

Junta de Andalucía (1991). *La Merced. Cuatro siglos de historia*. Editorial Artes Gráficas Girón. 114 pp

Lara Ródenas, M. J. (2005). *Biografía de una iglesia: la parroquia de la Concepción de Huelva*. Colegio Oficial de Arquitectos de Huelva, 139 pp

Rodríguez López, J. (1991). *Isla Cristina en La Higuerita: recopilación de noticias, con comentarios, publicadas en "La Higuerita de tiempo pretérito y recuerdos*". Isla Cristina, 144 pp

Sugrañes Gómez, E. J. (1998). *La Milagrosa y las Hijas de la Caridad en Huelva*. Editorial Jiménez S.L., 187 pp


those obtained by the Instituto Portugues do Mar e Atmósfera (IPMA) for other sites not included in our documents (Batlló et al. 2012), these values are reported in Table S1 with an asterisk. The total number of sites with intensity values is 746.

## 3. Largest Intensities

A detailed description of damages corresponding to sites with largest intensity values is given in the *Supplementary Material*, here we summarized this information. The maximum intensity value has been assigned to Fonte dos Luzeiros, a small town in Algarve (South Portugal), which was almost totally destroyed by the earthquake (of the 16 houses only one was not destroyed: P1, P3, P5, P7, P6, P9, P11, references from Table 1) (Fig. 2a). We have assigned to this town an intensity value VIII–IX (EMS-98) (Fig. 3a, b).

There is a second group of sites in south Portugal, with maximum intensity VIII: Aljezur, Barao de S. Joao, Barao de S. Miguel, Benisafrim the largest town seriously affected with about 1700 inhabitants at that time), Cacela, Fuseta and Vila do Bispo. A third group of towns have been evaluated with maximum intensity VII–VIII. They are Castro-Marim, Lagos, Sagres and Tavira, a town with important historical buildings, which were seriously affected by the shock.

We have assigned maximum intensity VII to Estoi, Faro, Loulé and Portimao (Portugal), Beas and Isla Cristina (Fig. 2b) (SW Spain). Sites with assigned intensity VI–VII include Huelva, Ayamonte, Palos de Moguer in SW Spain and in SW Portugal the monastery of Batalha, Santa Quiteria Church (Meca), and Setúbal.

There are many cities and towns with intensity VI. We summarized the damage in large cities in Portugal (Lisbon), Spain (Seville) and Morocco (Rabay and Salé). In Lisbon 58–60 people were injured, cracks in many houses, Hospital of S. José, Church of Luz (large crack and risk of collapse), Paços do Concelho, school of Bellas Artes, fall of chimneys, statues and roofs. In Seville 3 people died for cardiac attacks and damage was reported in the Cathedral (Giralda tower), the *Torre del Oro* (Tower of Gold, Fig. 2c), the pillars of the dome and the Alcazar (cracks), as well as the partial collapse of some houses, walls, etc. In Morocco the largest intensity values correspond to Rabat and Salé (at 5 km from Rabat), 5 people died, 4 were injured and 6 old houses collapsed.

The total number of casualties due to the 1969 shock was 25 deaths, with more than 80 injured. In Spain 4 people died (3 in Seville and 1 in Badajoz, due to heart attacks and about 10 were injured. In Portugal 13 people died (11 directly due to the earthquake and 2 due to consequence of heavy injures suffered) and 58 injured. In Morocco 8 people died (3 in Safi, 2 in Salé, 2 in Chichaoua, 1 in Imi n'Tanoute) and more than 12 were injured. The high number of


Figure 2
Damage of the 1969 earthquake in Fonte Luzeiros, Portugal (**a**). Isla Cristina, Spain (**b**) and Seville, Spain (**c**)

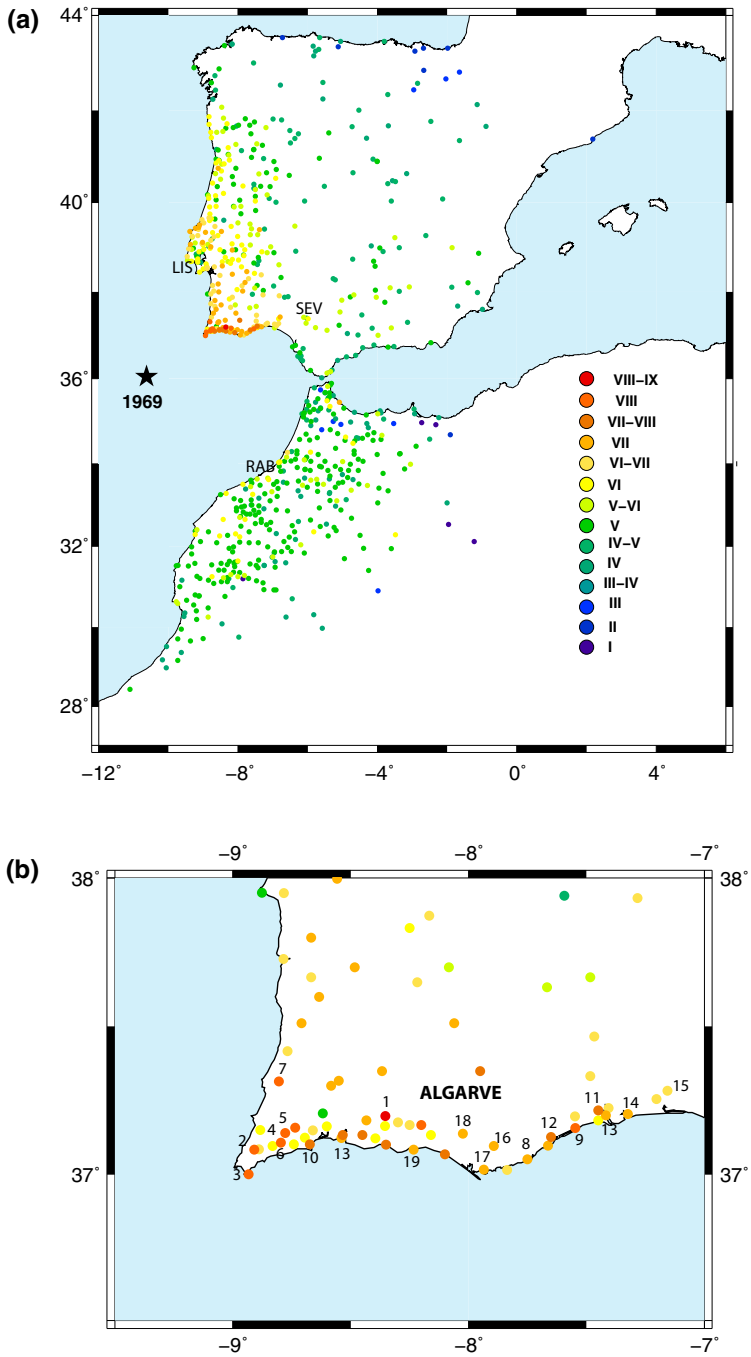


1.- Fonte dos Luzeiros 2.- Vila do Bispo 3.- Sagres 4.- B. S. Joao 5.- Bensafrim

6.- B. S. Miguel 7.- Aljezur 8.- Fuseta 9.- Cacela 10.- Lagos 11.- Castro Marim

12.- Tavira 13.- Lagos 14.- Isla Cristina 15.- Beas 16.- Estoi 17.- Faro

18.- Loulé 19.- Portimao

Figure 3

**a** New map of EMS-98 intensities for the 1969 earthquake. *LIS* Lisbon, *SEV* Seville, *RAB* Rabat. **b** Detail of new intensities on the SW Iberia

victims in Morocco, took place in areas where the maximum intensity was VI, and may be explained by the poor construction and the bad state of preservation of houses, according to the documents the deaths occurred in old houses (MEM, M1, M2, M3).

## 4. Intensity Map

In Fig. 3a and b and Table S1 (Supplementary Material) we show the assigned intensity value for each site. We observe that the largest intensity values (VII–VIII to VIII–IX) are in the southernmost coast of the Algarve region (Southern Portugal) along an E-W direction parallel to the coast located at epicentral distances between 200 and 320 km. However, at similar epicentral distance, but along the N-S coast of the Algarve, the intensity values are lower (for example at Faro or Sines both at 280 km). Further north, for example, in Lisbon (located at 340 km at NNE of the epicenter), the intensity value is VI, but in Castro-Marim (330 km), Santa Luzia (310 km) or Tavira (309 km), all located along the E-W southern coast the maximum intensity is VII–VIII. In Spain the higher intensities (VI–VII to VII) are in the Huelva region at the border with Portugal: in Isla Cristina (340 km, intensity VII), Huelva city (373 km, intensity VI–VII) and Ayamonte (334 km, intensity VI–VII),. In Morocco the distribution of intensities is very uniform; the maximum values are (VI) in Rabat-Salé (450 km) similar to those of Seville at the same epicentral distance.

In Fig. 4 we have plotted the intensity versus distance together with the error bands We have carried out a logarithmic adjustment of these values, obtaining the following relation:

$$I = 30.72 - 4.15ln(R)$$

where R is the epicentral distance in km. Using the values plotted in Fig. 4, and assuming a circular distribution in the intensity map with radius the average distance, we have applied the methodology developed by Johnston (1996) to obtain the moment magnitude $M_w$. If we use the area defined by intensity III, we obtain $M_w$ = 7.4, clearly lower than $M_w$ = 7.8 estimated by Fukao (1973) and Grimison and Chen (1988) and $M_s$ = 7.8 estimated by López-Arroyo and Udías (1972). This result shows that Mw values obtained from isoseismal maps may be underestimated.

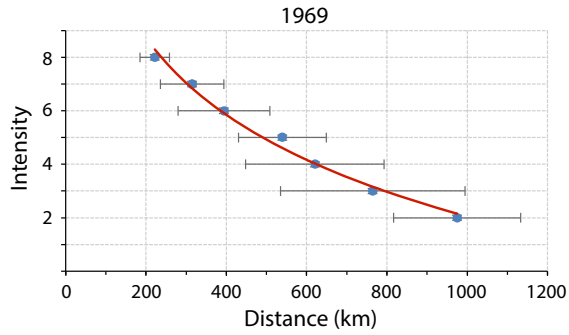


Figure 4
Attenuation of the 1969 new intensities versus distance

## 5. Hypocentral Relocation of the 1969 Seismic Sequence

The 1969 earthquake was followed by a long series of aftershocks lasting over a year. The Instituto Geográfico Nacional (IGN) estimated the hypocentral coordinates for the main event and aftershocks (Mézcua and Martínez Solares 1983). However, the distant and asymmetric distribution of seismic stations (all analogical instruments onshore), and the complex earth structure in this region, cause large uncertainties in hypocentral determination, especially, in focal depth. In fact, for more than 90% aftershocks with epicentral determination the focal depth could not be constrained (https://www.ign.es/web/ign/portal/sis-catalogo-terremotos) due to the low number of available P and S phases and the large azimuthal gaps.

In the last years, different 2D and 3D velocity models have been proposed for this region (Grandin et al. 2007; Sallarès et al. 2011, 2013; Martínez-Loriente et al. 2013; Civiero et al. 2018; Lozano et al. 2019 under revision). The development of non linear methods for hypocentral determination, such as the NonLinLoc (NLL) software (Lomax et al. 2000; http://alomax.free.fr/nlloc/), and the use of 3D models, are powerful tools to improve the hypocentral parameter. This method performs a non-linear probabilistic search of an earthquake hypocenter, allowing

travel-time calculation within a 3-D grid. The main advantage of this non-linear location is that it represents a complete, probabilistic solution of the location problem and calculates the posterior probability density function (PDF), which provides more reliable location uncertainties than classical linearized inversions (Tarantola and Valette 1982). Therefore, this method allows identifying multiple optimal solutions within irregular confidence volumes.

We have used the NLL software and an extended version of the 3D P-wave velocity model (Lozano et al. 2019 under revision) to relocate the 1969 main shock and aftershocks. This model was interpolated from a velocity-depth database retrived from the most significant published 2-D seismic velocity models from active seismic profiles surveys carried out in the SW Iberia margin. We have extended the 3-D model propose by Lozano et al. (2019, under revision) to the rest of the Iberian Peninsula using the IGN 1-D continental-crust model (Mézcua and Martínez Solares 1983) and a 1-D homogeneous layered model for the Alboran domain based on recent local tomography studies (Stich et al. 2003; Grevemeyer et al. 2015). The new 3D P-wave velocity model (Fig. 5) covers the region from latitude 33°N to 44°N, and longitude 15°W to 4°E and down to 80 km depth. For upper-mantle depths, we have considered a laterally heterogeneous velocity distribution using three different 1-D layered models: a constant P-wave velocity of 8.15 km/s for the oceanic domain (Laske et al. 2013; Custodio et al. 2015), a local velocity model modified from Silva et al. 2017 for the Gulf of Cadiz region, and the IASP-91 global model (Kennett and Engdahl 1991) for the Iberian Peninsula which assumes a smooth velocity gradient from 8.0 km/s at the Moho.

For the relocation with NLL we generated a regional 1761 × 1241 × 80 $km^3$ grid volume with 1 km spacing interpolated using a kriging algorithm from the original 3D velocity model and assumed a "2flat-earth" approach. For the inversion, the depth search was set free to oscillate in the whole depth range and we assumed a constant average $v_p/v_s$ ratio of 1.74, obtained using the Wadati diagram with a set of representative $M > 3$ earthquakes registered in the region for the period 2007–2018.

We have relocated the main shock and a selection of 24 aftershocks from the IGN catalogue occurred in the period from 28 February to 31 December 1969, recorded at the regional seismological stations from Spanish, Portuguese and Moroccan networks (Fig. 6a). We only considered those earthquakes recorded at least by 8 seismic stations and with a minimum of 8 P phases and 4 S phases. For the main shock we used 12 P-wave readings, since no S-wave were available, and for the largest aftershock 10 P-wave and 2 S-wave readings. Data corresponds to the IGN original bulletins, original readings (taken from seismograms) of P and S-waves by López-Arroyo and Udías (1972) and some additional data. During the relocation process, phases with residuals larger than 2.5 s were considered outliers and removed. In Table 4 we show the relocated hypocenters and error parameters (RMS of travel time residuals, depth errors and the semi-axes of the 90% confidence 2-D error ellipsoid). Maximum likelihood hypocenters as well as the probability density functions (PDF) are plotted in Fig. 6b. The location PDFs are large and highly irregular, mainly due to the fact that all earthquakes are located outside the network, far away from land stations (distance to the closest station over 300 km), and with significant azimuthal gaps (over 240°) (Lomax et al. 2000, 2009). Results must be taken with caution, since they may be strongly affected by the poor station distribution, the scarce number of phases used for location, and the use of a "flat-earth" approximation, resulting in large depth uncertainties.

From Fig. 6b, where we have also plotted the epicenters taken from the IGN catalogue, we observe that now the relocated main shock (the red star) is closer to the coast (black star is the IGN catalogue epicenter) and deeper (37 km versus 20 km). Fukao (1973) obtained focal depths of 16 km or 33 km for the main shock, and of 40–45 km for aftershocks. Grimison and Chen (1988) estimated a depth of 31 km for the main shock and 50 km for the largest aftershock (versus 37 km in our study). Other reported focal depths for main shock, varies from 10 km (US Geological Survey Catalogue), 19 km (ISC Catalogue) or 21 km (Centenial Catalogue, Engdahl et al. 1998; and Villaseñor and Engdahl 2005). Most aftershocks relocated in this study (red

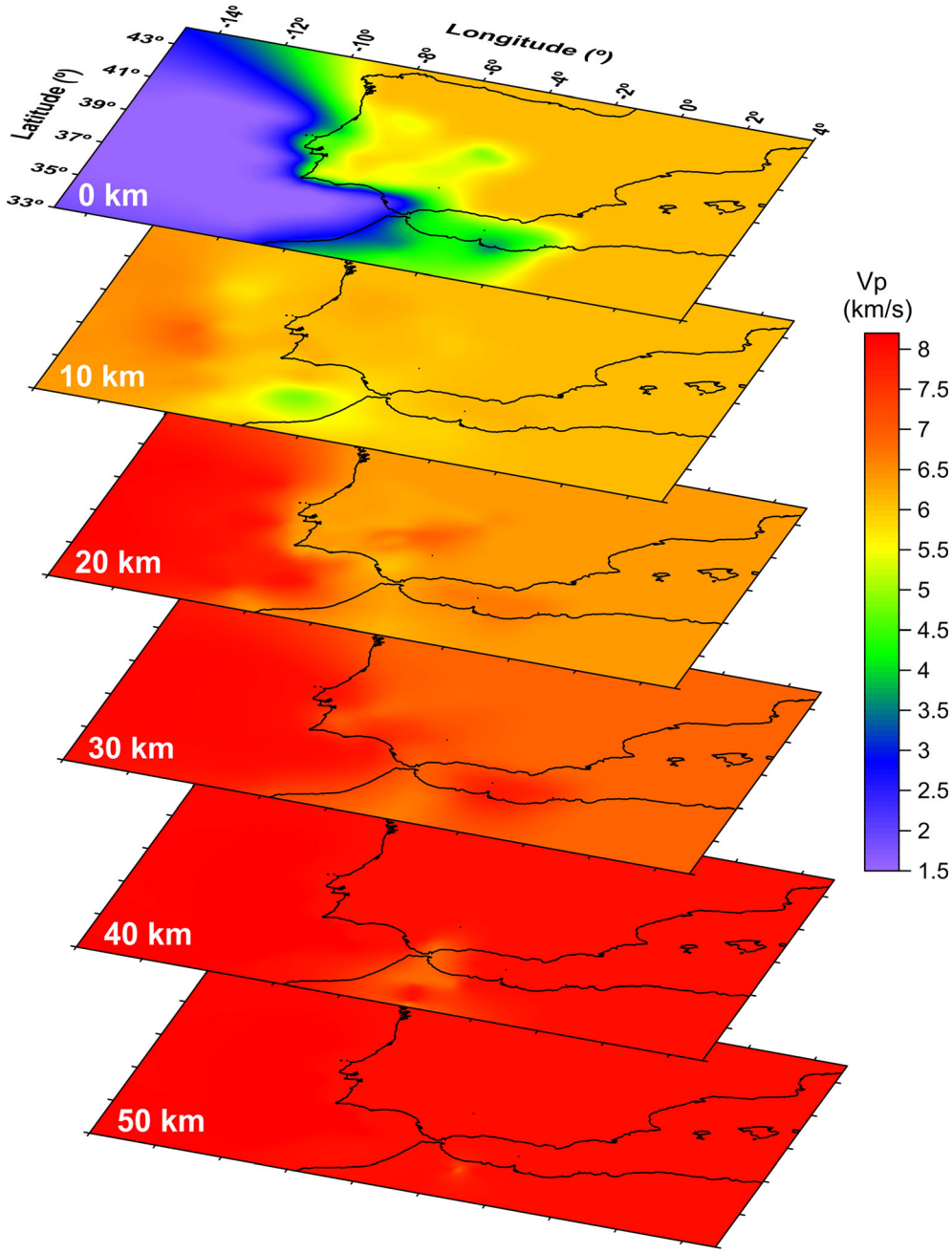


Figure 5
3-D velocity model used on this study

circles) are in a depth range between 30 and 40 km (19 events), with only three earthquakes deeper than 55 km (Table 4). No earthquakes have been located at depths shallower than 30 km. In the IGN catalogue (black crosses in Fig. 6b), depth parameter was not constrained, except for one aftershock. This range of focal depths is in good agreement with results obtained for other earthquakes in this region. For example, the 2007 ($M_w$ = 6.0) and 2009 ($M_w$ = 5.5) earthquakes, located in this region, have focal depth of 30–40 km

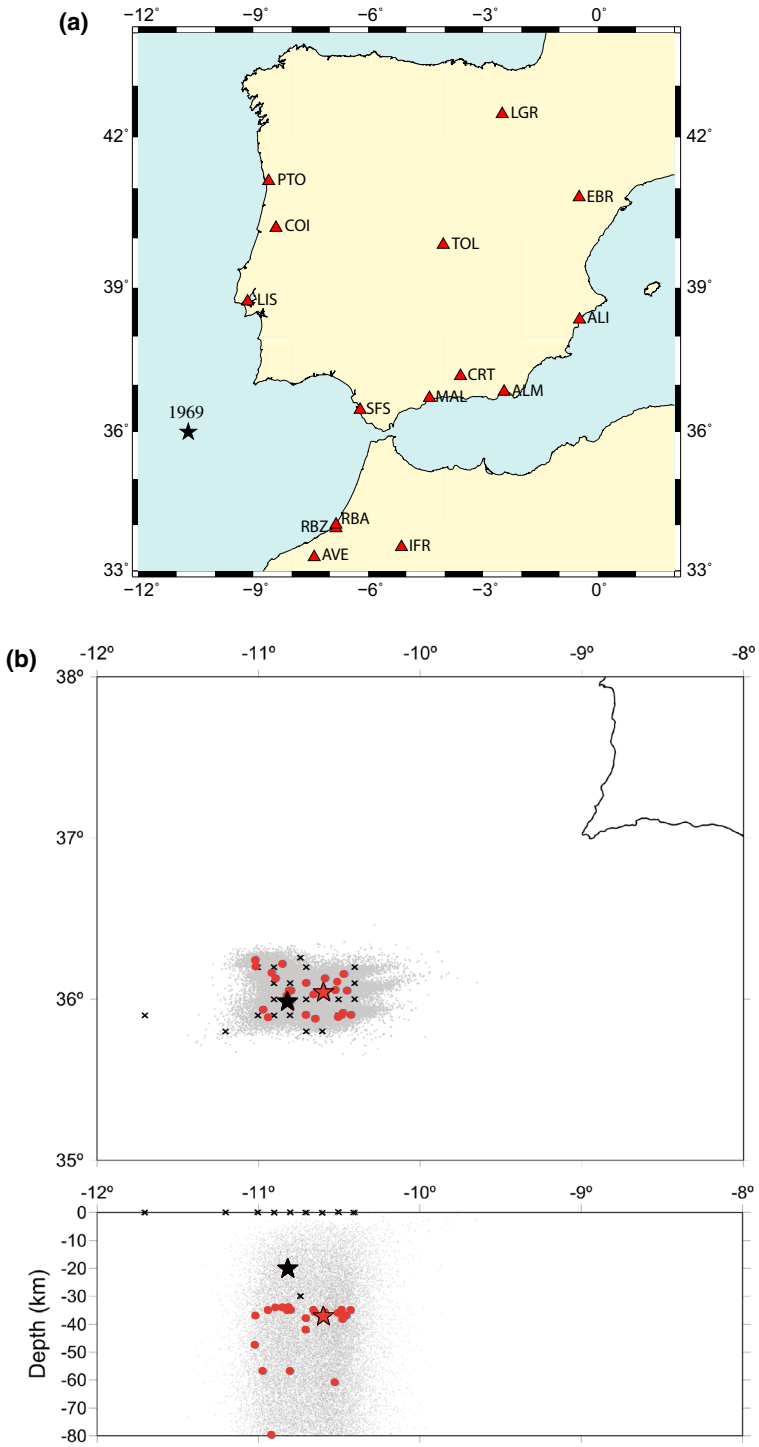


Figure 6

**a** Seismic stations in the Iberian Peninsula which recorded the 29 February 1969 earthquake and its aftershocks. **b** Relocation of 1969 aftershock series using NLL algorithm and a 3D structure model (Lozano et al. 2019, under revision). At top, distribution of epicenters for the 1969 main shock (black star previous solution, red star this study). Black crosses are the previous aftershocks and red circles relocated epicenters. At bottom, vertical cross section of hypocenters (symbols as top). The grey area shows the probability density functions

Table 4

*Relocated hypocentral parameters for the 1969 main shock and selected aftershocks*

| Date | Mag | Time | Lat. (°) | Lon. (°) | h (km) | RMS (s) | Errz (km) | Smajax (km) | Sminax (km) | Az(°) | Nphs |
|---|---|---|---|---|---|---|---|---|---|---|---|
| 1969/02/28 | 7.8[a] | 02:40:34.97 | 36.0429 | − 10.5923 | 37 | 0.52 | 37 | 37 | 8 | 19 | 12 |
| 1969/02/28 | 5.7 | 04:25:33.70 | 36.2054 | − 11.0141 | 37 | 0.87 | 35 | 44 | 18 | 16 | 12 |
| 1969/02/28 | 4.6 | 09:59:51.57 | 36.0548 | − 10.8087 | 34 | 0.90 | 34 | 26 | 13 | 13 | 13 |
| 1969/02/28 | 4.2 | 15:20:42.79 | 36.0310 | − 10.6541 | 35 | 1.00 | 30 | 30 | 12 | 16 | 16 |
| 1969/02/28 | 3.6 | 16:21:02.21 | 36.1023 | − 10.7006 | 38 | 1.03 | 31 | 28 | 10 | 11 | 15 |
| 1969/02/28 | 4.2 | 18:24:38.79 | 36.0548 | − 10.7948 | 35 | 0.86 | 32 | 26 | 9 | 10 | 13 |
| 1969/03/01 | 4.1 | 22:07:53.72 | 35.9042 | − 10.7014 | 42 | 0.91 | 33 | 22 | 9 | 9 | 17 |
| 1969/03/02 | 4.4 | 18:00:59.73 | 36.1658 | − 10.9138 | 80 | 0.74 | 34 | 17 | 7 | 8 | 23 |
| 1969/03/05 | 4.7 | 02:57:36.21 | 35.9874 | − 10.7973 | 57 | 0.50 | 33 | 18 | 5 | 14 | 17 |
| 1969/03/06 | 4.8 | 19:23:44.00 | 36.1301 | − 10.8904 | 34 | 0.62 | 32 | 17 | 7 | 14 | 18 |
| 1969/03/07 | 4.3 | 21:31:16.75 | 36.1578 | − 10.4674 | 37 | 0.68 | 30 | 26 | 6 | 9 | 16 |
| 1969/03/08 | 4.2 | 03:36:00.47 | 35.9161 | − 10.4730 | 38 | 0.76 | 29 | 15 | 8 | 18 | 18 |
| 1969/03/09 | 4.5 | 13:08:16.05 | 36.2212 | − 10.8479 | 34 | 0.88 | 30 | 17 | 7 | 8 | 24 |
| 1969/03/10 | 3.9 | 09:56:50.44 | 35.8903 | − 10.5026 | 36 | 0.73 | 26 | 16 | 5 | 13 | 25 |
| 1969/03/12 | 3.7 | 03:11:35.26 | 36.1301 | − 10.5840 | 36 | 0.72 | 32 | 18 | 8 | 4 | 16 |
| 1969/03/18 | 4.2 | 04:17:37.11 | 36.0310 | − 10.5846 | 37 | 0.94 | 33 | 18 | 10 | 17 | 17 |
| 1969/03/18 | 4.0 | 06:00:36.32 | 35.9042 | − 10.4236 | 35 | 0.80 | 28 | 24 | 6 | 12 | 18 |
| 1969/04/10 | 4.2 | 16:52:06.58 | 35.9042 | − 10.4792 | 35 | 0.68 | 29 | 16 | 7 | 10 | 16 |
| 1969/05/05 | 5.5 | 05:34:24.85 | 36.0568 | − 10.5201 | 61 | 0.83 | 31 | 15 | 6.5 | 13 | 24 |
| 1969/05/10 | 4.3 | 13:31:14.82 | 36.2450 | − 10.0169 | 48 | 0.64 | 33 | 16 | 7.0 | 7 | 20 |
| 1969/08/03 | 4.1 | 02:53:07.55 | 35.8804 | − 10.6443 | 36 | 0.75 | 34 | 23 | 12.5 | − 6 | 16 |
| 1969/08/08 | 4.2 | 20:02:35.75 | 35.9359 | − 10.9675 | 57 | 0.96 | 33 | 22 | 12.4 | 7 | 16 |
| 1969/10/18 | 4.2 | 05:31:45.68 | 36.0231 | − 10.8205 | 35 | 0.64 | 32 | 24 | 10.8 | − 6 | 14 |
| 1969/11/05 | 4.6 | 07:47:34.73 | 35.8883 | − 10.9364 | 35 | 0.85 | 29 | 19 | 8.4 | 19 | 19 |
| 1969/12/24 | 5.1 | 05:04:46.79 | 36.0548 | − 10.4469 | 37 | 0.69 | 32 | 20 | 10.0 | 3 | 13 |

[a]Moment magnitude $M_w$

*Az* azimuth, *Nphs* number of phases

and the same happens for hypocenter locations obtained for other earthquakes occurred in this region in the NEAREST project (Stich et al. 2005, 2007; Geissler et al. 2010; Custodio et al. 2012; Pro et al. 2013; Silva et al. 2017; Lozano et al. 2019 under revision). The lack of seismic foci at shallow depths (less than 30 km) and the distribution of the 1969 sequence with shocks below 30 km depth may be explained due to the release of stress at that depth due to the existence there of exhumed mantle rocks, with rigid and cool material (Martínez-Loriente et al. 2013).

In Fig. 7 we show the uncertainties in the relocations. In general, the origin times are well estimated, with most RMS travel time residuals in the range of 0.6–1.0 s (Table 4 and Fig. 7). The 2-D confidence ellipse provided by NLL represents an accurate image of the uncertainties. Epicentral errors (Smajax and Sminax) vary from 14 to 30 km and 5 to 1 km respectively. From Table 4 we can also observe that most ellipse-error azimuths are oriented almost N–S (between − 6° and 19°). So, we can conclude that the epicenters are better located in longitude than in latitude due to the poor geometry of the stations network. The use in the hypocentral determinations of a non-linear probabilistic location method has provided more accurate solutions, in spite of the large focal depths errors (of the order of 25–35 km).

In Fig. 8 we have plotted the aftershock sequence versus time, starting on 28 February. Data are taken from López-Arroyo and Udías (1972)and correspond to events recorded, although the epicenters could not be determined due to the low number of seismic phases available. A total of 422 events were identified as aftershocks until 31 December 1969, the same period used in the hypocenter relocation. Number of events versus time shows that most earthquakes occurred during the first 10 days after the main shock (172 earthquakes).

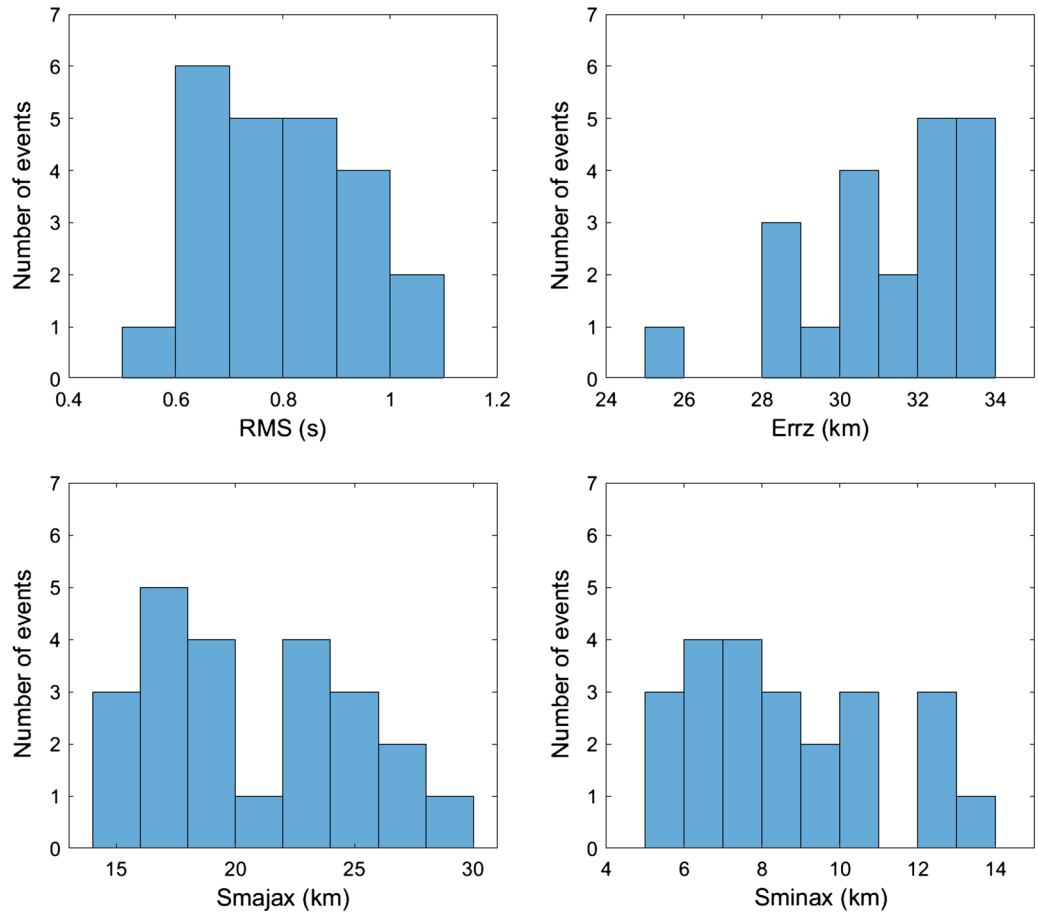


Figure 7
Histograms of errors for time origin (rms), depth (errz) and semi-axes of error elipses for epicenters

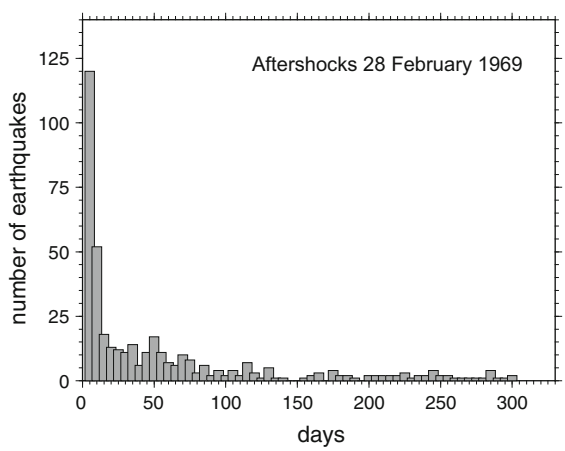


Figure 8
Number of earthquakes versus time for the 1969 seismic series

### 6. *Comparison Between the 1969 and the 1755 Lisbon Earthquake*

The 1969 earthquake occurred in the same region as the 1755 Lisbon earthquake (Fig. 1b). For the Lisbon 1755 event there are many unsolved questions such as its hypocenter location or its rupture process. However, for both earthquakes, the 1755 and 1969, we have detailed information on the intensity values in the Iberian Peninsula, so that we can compare their intensity maps and from them to draw some conclusions about the similarity or dissimilarity of their rupture process.

In Fig. 9 we have plotted the intensity values for the 1755 event in the Iberian Peninsula taken from Martínez Solares (2001) for Spain and from AHEAD,

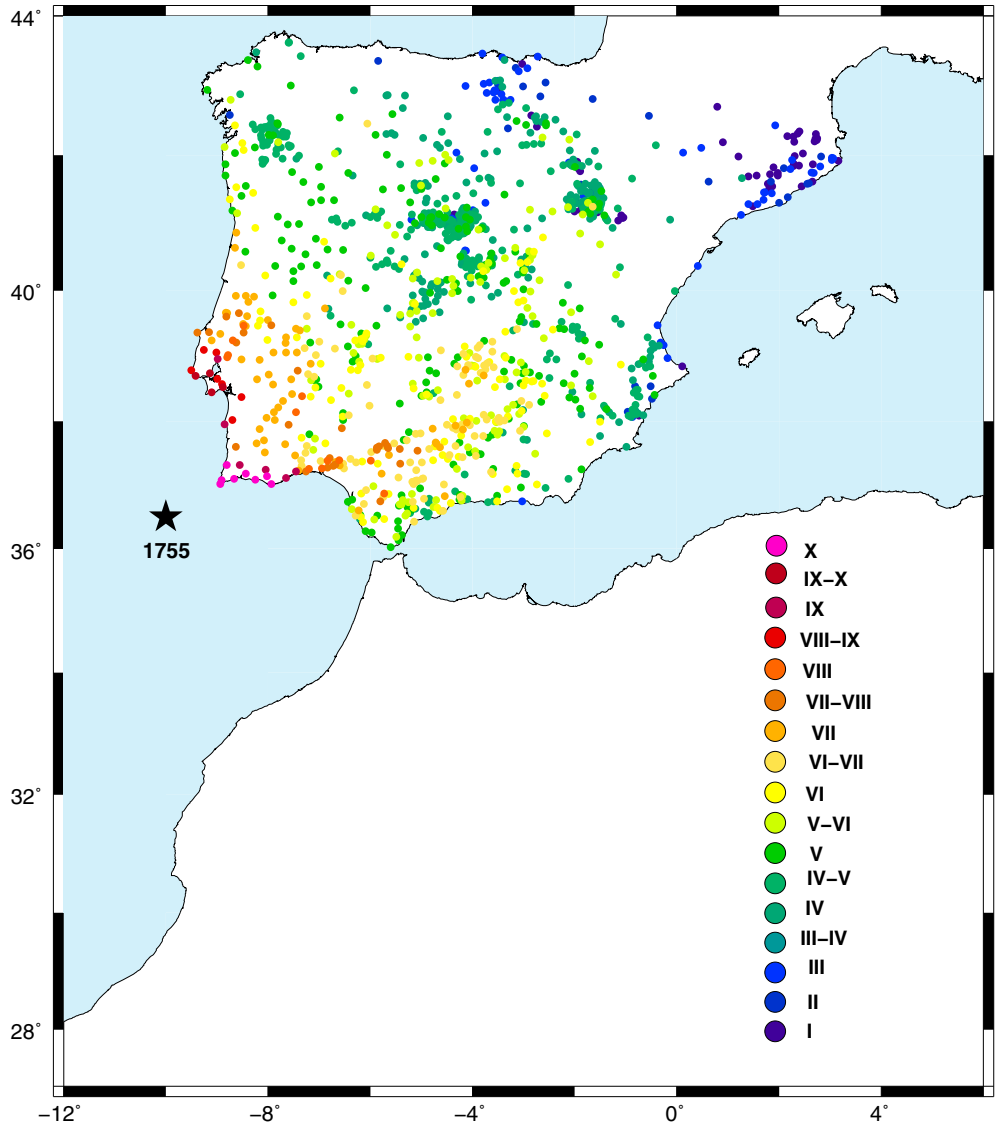


Figure 9
Intensity map for 1755 earthquake. Values from Spain are taken from Martínez-Solares (2001) and from Portugal form AHED

European Archive of Historical EArthquake Data (https://www.emidius.eu/AHEAD) for Portugal. Unfortunately no data are available for Morocco, so the comparison between both shocks will be limited to the Iberian Peninsula. When compare with the intensities distribution for the 1969 (Fig. 3) we observe important differences. For 1755 the largest intensities (X) are along the south of Portugal (the Algarve N-S coast) and in the Lisbon region, with intensities of IX and IX–X. For the 1969 event, the largest intensities are in southern Portugal, along the Algarve E-W coast (VIII to VIII–X) and lower intensities (VI–VII) in the Lisbon region). Another important difference concerns the epicenters: the 1755 event is supposed to be located (Martínez Solares and López Arroyo 2004) closer to the coast than the 1969 (150 km from Saint Vincent Cape for 1755 event versus 220 km for the 1969). However, this difference alone seems not to be sufficient to justify the different intensity pattern of the two earthquakes.

Based on these differences we explore what could have been the rupture process for the 1755 event. For the 1969 earthquake, the focal mechanism is well determined using different data and methodologies, and it corresponds to reverse faulting motion with planes oriented in E-W direction. The dimension of the rupture has been estimated 85–90 km (Fukao 1973; López-Arroyo and Udías 1972; Grimison and Chen 1988) in agreement with the spatial extension of our relocated aftershocks (Fig. 6b). López-Arroyo and Udías (1972) and Fukao (1973) have observed directivity effects using surface waves. The intensities distribution suggests that the rupture occurred along an E-W plane (Fig. 1b) propagating to the east toward the Strait of Gibraltar. This explains that the higher intensity values were reached in southern Portugal (E-W Algarve coast, Fig. 3). The different intensities distribution for the 1755 suggests also a different source rupture process. To explain this process we consider the earthquake occurred the 2009 ($M_w$ = 5.5) very close to the proposed 1755 epicenter. For this earthquake Pro et al. (2013) have proposed that the rupture occurred in a NE-SW vertical plane propagating to the NE (in the direction from Saint Vincent Cape to Lisbon, Fig. 1b). The location and focal mechanism of the 2009 earthquake differ from those of the 1969, suggesting that the 2009 event could be an alternative, potential candidate to explain the rupture process of the 1755.

In order to check this hypothesis, we have carried out a comparison between synthetic and intensity-based PGAs for the 1755 and 1969 earthquakes. The intensity-based PGA values have been obtained using Faenza and Michelini (2010) (this relation has been used recently by the IGN (2013) to update the seismic hazard maps in Spain):

$$I = 1.68 + 2.58log(PGA) \quad (1)$$

Using this relation, the 1755 event reached a peak value of 1.7 g, with the highest values along the Southern coast of Portugal and the western coast close to Lisbon. However, using the same relation, the largest PGAs values for 1969 earthquakes (0.4 g) were confined only in the southern coast (Algarve). In Fig. 10 we have plotted the PGA ratios $r_{PGA}$, defined as the ratio of the PGAs for the 1755 and 1969 earthquakes.

$$r_{PGA} = PGA_{1755}/PGA_{1969} \quad (2)$$

We have computed $r_{PGA}$ for each site where intensity values are available for both earthquakes within a radius of 2 km. We use warm (red) and cold (blue) colors denote respectively positive and negative anomalies of the PGA ratio with respect to its median value. Positive anomalies (red color), meaning that intensities of 1755 are larger than the corresponding of 1969, are found in the Lisbon and surrounding area, and in the N-S coast of the Algarve region, (S. Portugal) near Saint Vincent Cape (SVC). These spatial anomalies cannot be attributed to local site effects, which cancel out by considering the ratio of PGAs at the same site, and must be instead attributed to a differences in the radiation pattern of the two earthquakes, either controlled by differences in the epicentral location, depth, focal mechanism and/or directivity. This observation suggests that the location and rupture mechanism of the 1755 earthquake differed from those of the 1969 earthquake.

We used the *pyrocko* library (Heimann et al. 2017) to estimate theoretical PGA values at those sites where seismic intensities estimations are available; a similar procedure has been used by Buforn et al. (2015) and Dahm et al. (2018) for different earthquakes. Full waveform synthetic 3-components accelerations have been computed at all these sites, simulating two earthquake scenarios, using a global velocity model (AK135). In the first scenario, we simulate the 1755 earthquake assuming location, depth, magnitude and focal mechanism of the 1969 earthquake and in the second under the assumption that its location and mechanism correspond to those of the 2009 earthquake (Table 5). For both simulations, finite rupture processes are ignored, as there is no reliable information on the rupture directivity of these earthquakes. We consider in both cases a spatial point-source with 30 s rupture duration, to simulate waveforms with compatible frequency content. PGAs are here computed as the geometrical mean of the maximum acceleration of horizontal components. Figure 11 shows the ratio of the normalized PGAs computed for the 1969 and 2009 scenarios (warm and cold colors represent positive and negative deviations for the median ratio). We observe that the largest anomalies, that is, the differences between the two

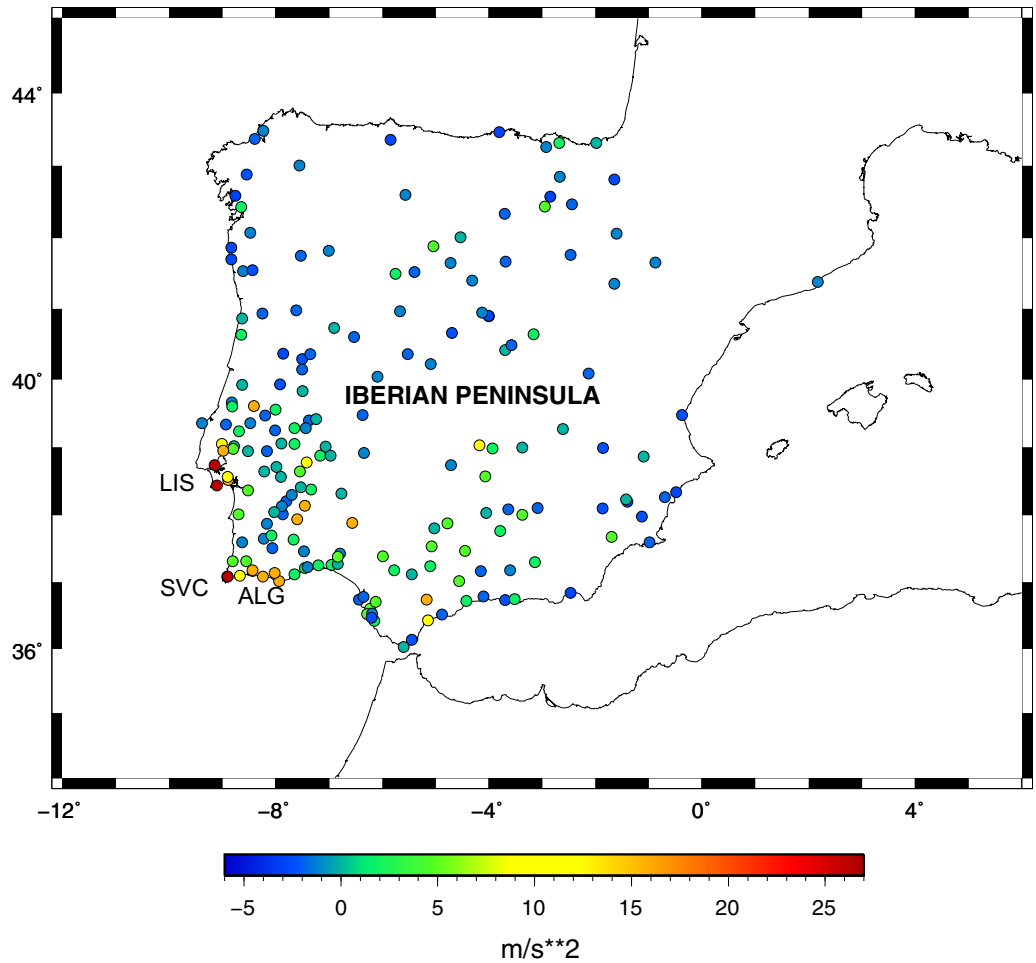


Figure 10
Map of the PGA ratio, $r_{PGA}$, between the 1755 and 1969 earthquake. Red color sites along the Western Portugal coast indicate anomalous large acceleration for the 1755 earthquake, with respect to the 1969 earthquake

Table 5

*Focal parameters*

| Date | Time | Lat. (°) | Lon. (°) | h (km) | $M_0$ (Nm) | Str/dip/rake (°) | $M_w$ |
|---|---|---|---|---|---|---|---|
| 28-02-1969 | 02:40: 34 | 36.0469 | − 10.6273 | 31 | $6 \times 10^{20}$ | 231/47/54 | 7.8 |
| 17-12-2009 | 01:37:49 | 36.4702 | − 10.0318 | 36 | $2.5 \times 10^{17}$ | 217/89/− 58 | 5.5 |
| 01-01-1755 | 10:16:00 | 36.50 | − 10.0 | – | – | – | – |

scenarios, are at the Lisbon region, with positive anomalies also present along the Western coast of Portugal. In both cases intensities deviations from the median indicate that intensities are higher for the 2009 than for the 1969 scenarios. We can then conclude that the intensity distribution of 1755 earthquake is more similar to that of the earthquake of 2009 than to the one of 1969. Therefore the distribution of intensities of the 1755 Lisbon earthquake can be better explained assuming that it took place close to the location of the 2009 earthquake and with a similar mechanism, with a reverse faulting rupture

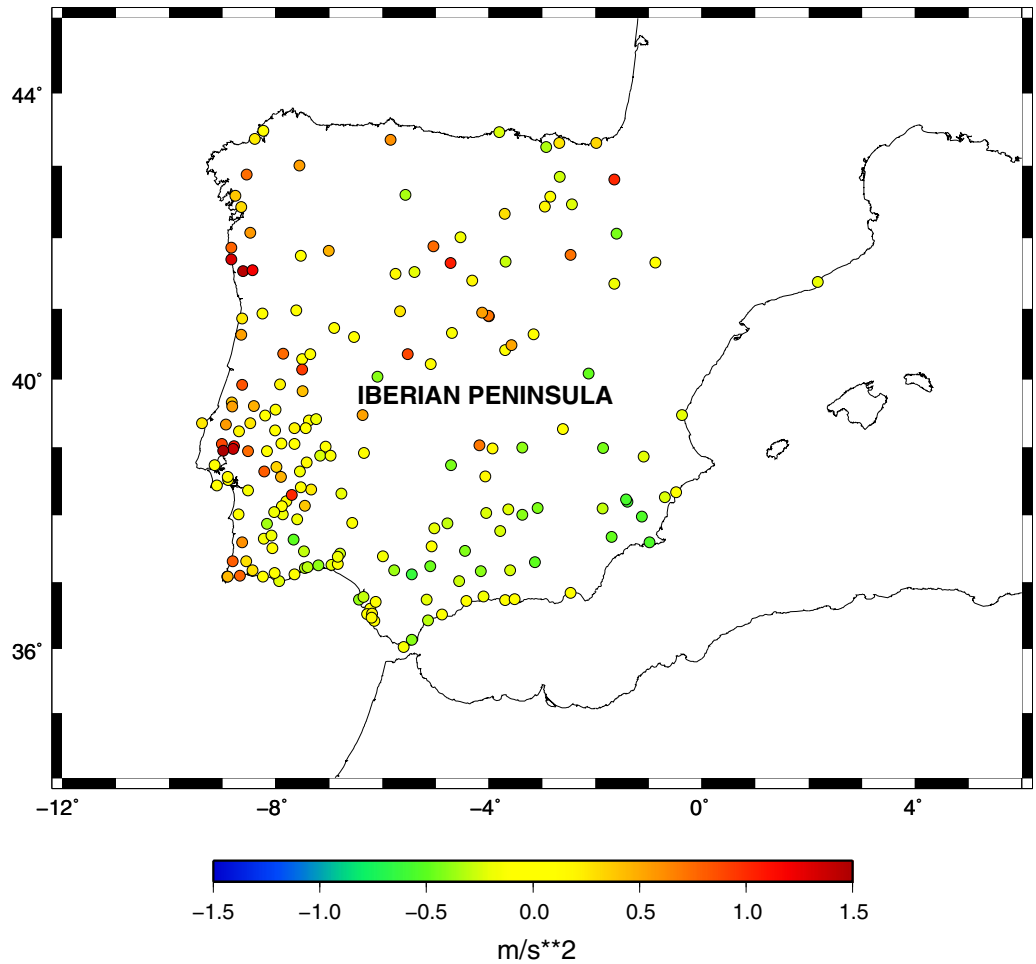


Figure 11
Map of the normalized synthetic PGA ratio for 1755 earthquake, $r_{PGA}$, between the 2009 and 1969 scenarios. Values are plotted as deviations from the median $r_{PGA}$, with warm and cold colors representing positive and negative deviations

on a nearly vertical plane in the NE-SW direction and propagating toward the NE.

## 7. *Conclusions*

- A new intensity map has been obtained for the 1969 earthquake for the Iberian Peninsula and northern Morocco using original documents some of them not used previously. The comparison between this map and the 1755 intensity map shows a different distribution; while for the 1969 event the largest intensities are found in southern Portugal (E-W coast of Algarve), for the 1755 the maximum intensities are more to the north in the N-S coast of Algarve and in the Lisbon region (NE from the epicenter). The 1969 maximum intensities in southern Portugal can be explained by the rupture process, with reverse motion as given by its mechanism and the rupture propagating in E-W direction parallel to the coast toward the Strait of Gibraltar. This rupture is not compatible with the distribution of intensities for the 1755 earthquake.
- The relocation of the main shock and 24 larger aftershocks, show focal depths mostly between 30 and 50 km in agreement with results obtained in other studies which confirms that the seismic activity in the Saint Vincent Cape occurs in an

anomalous upper mantle. The spatial distribution of aftershocks is located along an E-W band with less than 30 km width.

- Synthetic PGAs values were generated for the 1755 earthquake using two possible rupture scenarios, namely, with hypocenter and focal mechanism as the 1969 event or as the 2009 earthquake. The comparison between the distribution of synthetic and intensity-based of PGA values shows that the second scenario reproduces better the observed intensities. Based on these results we propose the location and focal mechanism of the 2009 earthquakes as better estimates for the 1755 Lisbon earthquake. However, it is important to remember that for the Lisbon earthquake the only available data are the intensities derived from documented damages and consequently all derived parameters are only estimates.

## *Acknowledgements*

This work has been partially supported by the Spanish Ministerio de Economia, Industria y Competitividad, project CGL2017-86097-R.



## References

Baptista, M. A., Miranda, P. M. A., Miranda, J. M., & Mendes-Victor, L. (1998). Constrains on the source of the 1755 Lisbon Tsunami inferred from numerical modelling on historical data on the source of the 1755 Lisbon Tsunami. *Journal of Geodynamics, 25,* 159–174.

Batlló, J., Carrilho, F., Alves, P., Cruz, J. & Locati, M. (2012). A new online intensity data point database for Portugal. In *Proc. 15th World Conf on Earthq Eng,* Lisbon, Portugal. Accessible online https://www.iitk.ac.in/nicee/wcee/article/WCEE2012_3683.pdf.

Buforn, E., Pro, C., Sanz de Galdeano, C., Cantavella, J. V., Cesca, S., Caldeira, B., Udías, A., & Mattesini, M. (2017). The 2016 south Alboran earthquake ($M_w$ = 6.4): A reactivation of the Ibero-Maghrebian region? *Tectonophysics, 712–713,* 704–715. https://doi.org/10.1016/j.tecto.2017.06.033.

Buforn, E., Sanz de Galdeano, C., & Udías, A. (1995). Seismotectonics of the Ibero-Maghrebian región. *Tectonophysics, 248,* 247–265.

Buforn, E., Udías, A., & Colombás, M. A. (1988). Seismicity, source mechanism and tectonics of the Azores-Gibraltar plate boundary. *Tectonophysics, 152,* 89–118.

Buforn, E., Udías, A., Sanz de Galdeano, C., & Cesca, S. (2015). The 1748 Montesa (southeast Spain) earthquake—A singular event. *Tectonophysics, 664,* 139–153.

Carranza, M. (2016). *Sistema de Alerta Sísmica temprana para el sur de la Península Ibérica: Determinación de los parámetros de la alerta.* Doctoral Thesis. Universidad Complutense de Madrid.

Cherkaoui, T. E. (1991). *Contribution a l'etude de l'alea sismique au Maroc*. Ph.D. Dissertation Université Joseph Fourier, Grenoble.

Civiero, C., Strak, V., Custódio, S., Silveira, G., Rowlinson, N., Arroucau, P., et al. (2018). A common deep source for upper-mantle upwelling below the Ibero-western Maghreb region from teleseismic P-wave travel-time tomography. *Earth and Planetary Science Letters, 499,* 157–172.

Custodio, S., Cesca, S., & Heimman, S. (2012). Fast kinematic waveform inversion and robustness analysis: Application to the 2007 Mw 5.9 Horseshoe Abyssal Plain Earthquake Offshore Southwest Iberia. *Bulletin of the Seismological Society of America, 102,* 361–376. https://doi.org/10.1785/0120110125.

Custodio, S., Dias, N. A., Carrilho, F., Gongora, E., Rio, I., Marreiros, C., et al. (2015). Seismology Earthquakes in western Iberia: improving the understanding of lithospheric deformation in a slowly deforming region. *Geophysical Journal International, 2015*(203), 127–145. https://doi.org/10.1093/gji/ggv285GJI.

Dahm, T., Heimann, S., Funke, S., Wendt, S., Rappsilber, I., Bindi, D., et al. (2018). Seismicity in the block mountains between Halle and Leipzig, Central Germany: centroid moment tensors, ground motion simulation, and felt intensities of two M ≈ 3 earthquakes in 2015 and 2017. *Journal of Seismology, 22*(4), 985–1003.

Engdahl, R., van der Hilst, R., & Buland, R. (1998). Global teleseismic earthquake relocation with improved travel times and procedures for depth determination. *Bulletin of the Seismological Society of America, 88,* 722–743.

Faenza, L., & Michelini, M. (2010). Regression analysis of MCS intensity and ground motion parameters in Italy and its application in ShakeMap. *Geophysical Journal International, 180,* 1138–1152. https://doi.org/10.1111/j.1365-246X.2009.04467.x.

Fukao, Y. (1973). Thrust faulting at a lithosphere plate boundary: The Portugal earthquake of 1969. *Earth and Planetary Science Letters, 18,* 205–216.

Geissler, W. H., Matias, L., Stich, D., Carillho, F., Jokat, W., Monna, S., et al. (2010). Focal mechanisms for sub-crustal earthquakes in the Gulf of Cadiz from dense OBS deployment. *Geophysical Research Letters, 37,* L18309. https://doi.org/10.1029/2010GL044289.

Grandin, R., Borges, J. F., Bezzeghoud, M., Caldeira, B., & Carrilho, F. (2007). Simulations of strong ground motion in SW Iberia for the 1969 February 28 ($Ms$ = 8.0) and the 1755 November 1 ($M$ ~8.5) earthquakes—II. Strong ground motion simulations. *Geophysical Journal International, 171,* 807–822.

Grevemeyer, I., Gràcia, E., Villaseñor, A., Leuchters, W., & Watts, A. B. (2015). Seismicity and active tectonics in the Alboran Sea, Western Mediterranean: Constraints from an offshore-onshore seismological network and swath bathymetry data. *Journal of Geophysical Research: Solid Earth, 120,* 8348–8365. https://doi.org/10.1002/2015JB012073.

Grimison, N. L., & Chen, W. P. (1986). The Azores Gibraltar Plate boundary: Focal mechanisms, depth of earthquakes and their tectonic implications. *Journal of Geophyical Research, 91,* 2029–2047.

Grimison, N. L., & Chen, W. P. (1988). Source mechanisms of four recent earthquakes along the Azores—Gibraltar plate boundary. *Geophysical Journal, 92,* 391–401.

Heimann, S., Kriegerowski, M., Isken, M., Cesca, S., Daout, S., Grigoli, F., Juretzek, C., Megies, T., Nooshiri, N., Steinberg, A., Sudhaus, H., Vasyura-Bathke, H., Willey, T. & Dahm, T. (2017). *Pyrocko—An open-source seismology toolbox and library*. V. 0.3. GFZ Data Services. https://doi.org/10.5880/gfz.2.1.2017.001.

IGN. (2013). *Actualización de Mapas de Peligrosidad Sísmica de España*. Madrid: Centro Nacional de Información Geográfica.

Johnston, A. (1996). Seismic moment assessment of earthquakes in stable continental regions-111. New Madrid 181 1-1812, Charleston 1886 and Lisbon 1755. *Geophysical Journal International, 1996*(126), 314–344.

Kennett, B. L. N., & Engdahl, E. R. (1991). Traveltimes for global earthquake location and phase identification. *Geophysical Journal International, 105,* 429–465. https://doi.org/10.1111/j.1365-246X.1991.tb06724.x.

Laske, G., Masters, G., Ma, Z. & Pasyanos, M., (2013). Update on CRUST1.0 A 1-degree Global Model of Earth's Crust. In *Geophys. Res. Abstracts* (vol. **15**, pp. EGU2013-2658). EGU General Assembly 2013, http://igppweb.ucsd.edu/~gabi/crust1.html.

Levret, A. (1991). The effects of the November 1, 1755 Lisbon earthquake in Morocco. *Tectonophysics, 193*(1–3), 83–94.

Lomax, A., Michelini, A. & Curtis, A. (2009) Earthquake Location, Direct, Global-Search Methods. In: R. A. Meyers (Ed.) *Encyclopedia of Complexity and System Science*, Part 5 (pp. 2449–2473). New York: Springer. https://doi.org/10.1007/978-0-387-30440-3.

Lomax, A., Virieux, J., Volant, P., & Berge-Thierry, C. (2000). Probabilistic earthquake location in 3D and layered models. In C. H. Thurber & N. Rabinowitz (Eds.), *Advances in Seismic Event Location. Modern Approaches in Geophysics* (Vol. 18). Dordrecht: Springer.

López-Arroyo, A., & Udías, A. (1972). Aftershock sequence and focal parameters of the February 28th, 1969 earthquake of the Azores-Gibraltar fracture zone. *Bulletin of the Seismological Society of America, 62*(3), 699–720.

Lozano, L., Cantavella, J. J. & Barco, J. (2019). A new 3-D P-wave velocity model for the Gulf of Cadiz and adjacent areas derived from controlled-source seismic data: Application to non-linear probabilistic relocation of moderate earthquakes. *Geophysical Journal International* **(under revision)**.

Machado, F. (1966). Contribuiçao para o estudo do terramoto de 1 de Novembro de 1755, *Rev. Fac. Ciencias de Lisboa*. 2a Serie-C, XIV, fasc.1,. 19–31.

Martínez Solares, J. M. (2001). *Los efectos en España del terremoto de Lisboa*. Madrid: Instituto Geográfico Nacional.

Martínez Solares, J. M., & López Arroyo, A. (2004). The great historical 1755 earthquake. Effects and damage in Spain. *Journal of Seismology, 8,* 275–294.

Martínez Solares, J. M., Lopez Arroyo, A., & Mezcua, J. (1979). Isoseismal map of the 1755 Lisbon earthquake obtained from Spanish data. *Tectonophysics, 53,* 301–313.

Martínez-Loriente, S., Grácia, E., Bartolome, R., Sallarés, V., Connors, C., Perea, H., et al. (2013). Active deformation in old oceanic lithosphere and significance for earthquake hazard: Seismic imaging of the Coral Patch Ridge area and neighboring abyssal plains (SW Iberian Margin). *Geochemistry, Geophysics, Geosystems, 14,* 2206–2231. https://doi.org/10.1002/ggge.

McKenzie, D. (1972). Active tectonics of the Mediterranean region. *Geophysical Journal of the Royal Astronomical Society, 30,* 109–185.

Mézcua, J. (1982). *Catálogo general de Isosistas de la Península Ibérica*. Madrid: Instituto Geográfico Nacional.

Mézcua, J, Martínez Solares, J. M. (1983). *Sismicidad del area Ibero-Mogrebí.* Publicación 203. Madrid: Instituto Geográfico Nacional.

Moreira, V. S. (1984). *Sismicidade histórica de Portugal Continental*. Lisboa: Revista Instituto Nacional de Meteorologia e Geofísica.

Moreira, V. S. (1985). Seismotectonics of PortugaI and its adjacent area in the Atlantic. *Tectonophysics, 117,* 85–96.

Paula, A. O., & Oliveira, C. S. (1996). Evaluation of 1947–1993 Macroseismic information in Portugal using the EMS-92 scale. *Annali di Geofisica XXXIV, 5,* 1989.

Pro, C., Buforn, E., Bezzeghoud, M., & Udías, A. (2013). The earthquakes of 29 July 2003, 12 February 2007, and 17 December 2009 in the region of Cape Saint Vincent (SW Iberia) and their relation with the 1755 Lisbon earthquake. *Tectonophysics, 583,* 16–27. https://doi.org/10.1016/j.tecto.2012.10.010.

Sallarès, V., Martínez-Loriente, S., Prada, M., Gràcia, E., Ranero, C. R., Gutscher, M. A., et al. (2013). Seismic evidence of exhumed mantle rock basement at the Gorringe Bank and the adjacent Horseshoeand Tagus abyssal plains (SW Iberia). *Earth and Planetary Science Letters, 365,* 120–131. https://doi.org/10.1016/j.epsl.2013.01.021.

Sallarès, V., Gaillerb, A., Gutscherb, M. A., Graindorgeb, D., Bartoloméa, R., Gràcia, E., et al. (2011). Seismic evidence for the presence of Jurassic oceanic crust in the central Gulf of Cadiz (SW Iberian margin). *Earth and Planetary Science Letters, 311*(1–2), 112–123. https://doi.org/10.1016/j.epsl.2011.09.003.

Silva, S., Terrinha, P., Matias, L., Duarte, J., Roque, C., Ranero, C., et al. (2017). Micro-seismicity in the Gulf of Cadiz: Is there a link between micro-seismicity, high magnitude earthquakes and active faults? *Tectonophysics, 717*(2017), 226–241.

Stich, D., Batlló, J., Morales, J., Macià, R., & Dineva, S. (2003). Source parameters of the Mw = 6.1 1910 Adra earthquake (southern Spain). *Geophysical Journal International, 155*(2), 539–546. https://doi.org/10.1046/j.1365-246X.2003.02059.x.

Stich, D., Mancilla, F., & Morales, J. (2005). Crust-Mantle Coupling in the Gulf of Cadiz (SW-Iberia). *Geophysical Research Letters*. https://doi.org/10.1029/2005GL023098.

Stich, D., Mancilla, F., Pondrelli, S., & Morales, J. (2007). Source analysis of the February 12th 2007, Mw 6.0 Horseshoe earthquake: Implications for the 1755 Lisbon earthquake. *Geophysical Research Letters.* https://doi.org/10.1029/2007gl0300127.

Tarantola, A., & Valette, B. (1982). Generalized nonlinear inverse problems solved using the least squares criterion. *Reviews of Geophysics*, *20*(2), 219.

Udías, A., & López Arroyo, A. (1970). Body and surface wave study of the source parameters of the 15, 1964 Spanish earthquake. *Tectonophysics, 9,* 323–346.

Udías, A., López Arroyo, A., & Mezcua, J. (1976). Seismotectonic of the Azores-Alboran region. *Tectonophysics, 31,* 259–289.

Vilanova, S. P., Nunes, C. F., & Fonseca, J. F. (2003). Lisbon 1755: A case of triggered onshore rupture? *Bulletin of the Seismological Society of America, 93,* 2056–2068.

Villaseñor, A., & Engdahl, R. (2005). A digital hypocenter catalog for the international seismological summary. *Seismological Research Letters, 76,* 554–559.

http://alomax.free.fr/nlloc/.

https://www.emidius.eu/AHEAD.

http://www.ign.es/web/ign/portal/sis-catalogo-terremotos.

Zitellini, N., Chierici, F., Sartori, R., & Torelli, L. (1999). The tectonic source of the 1755 Lisbon earthquake and tsunami. *Annali di Geofisica, 42,* 49–55.

(Received July 18, 2019, revised September 20, 2019, accepted September 24, 2019, Published online October 15, 2019)